COMPUTATION OF FEL PROCESSES

S. Reiche
UCLA Department of Physics & Astronomy, Los Angeles, CA 90095-1547, USA

Abstract

The Free-Electron Laser process is the interaction between an electron beam and a co-propagating radiation field, resulting in a collective instability with an exponential growth of the radiation field and the current modulation in the electron bunch. Although analytical models can describe the fundamental FEL amplification, the complexity of the FEL process with a multi-particle system and the evolution of a radiation field demands numerical calculation.

To achieve optimum performance the numerical solvers for FEL codes are highly specialized, using alternative methods than standard PIC codes. This presentation describes the basic algorithm for FEL simulations and addresses in particular the problems and limitations of simulating the FEL process.

INTRODUCTION

The FEL process is a collective instability [1] where an electron beam interacts with a co-propagating radiation field, coupled by the transverse deflection due to a periodic magnetic field of an undulator or wiggler. The output of the Free-Electron Laser depends on a large parameter space of input parameters ranging from the field of the undulator field, to the quality and pulse length of the driving electron beam, to the fluctuation in the initial position of each electron. The numerics have to be precise to several orders of magnitude in the Fourier components of the current modulation and the amplitude of the radiation field.

With several Free-Electron Lasers planned or under construction [2] it is essential to predict the performance as accurately as possible. In the design phase analytical formulae [3] are efficient to find the design parameters of the FEL, then numerical simulations can evaluate the choice of these parameters and predict any additional change in the performance with respect to the analytical model.

Modelling of the FEL process is challenging due to the different scales of the process. On the one hand, the radiation and the electron beam have to be tracked for the undulator length, which can range between one and a few hundred meters. On the other hand, the simulation has to resolve electron motion well below the radiation wavelength, which can range down to 1 Ångstrom. The scale of up to 12 orders of magnitude makes the Particle-in-Cell approach impractical.

With the ongoing research of high-gain single pass Free-Electron Lasers [4] over the last 20 years, numerical codes have been developed. Most of the time they were limited by the available computer resources of their time and the wavelength of interest. Long wavelength FELs are easier to model because the stronger diffraction tends to "wash-out" finer details in the electron distribution and motion. But, for VUV and X-ray FELs the performance is more sensitive to the beam quality, in particular the beam emittance or external effects such as undulator wakefields [20] or errors in the undulator field [21]. In addition, the start-up from noise (SASE FEL) and the extension of the wavelength range due to harmonics have a growing interest.

Table 1: Free-Electron Laser simulation codes, showing the number of dimensions, ability to do time-dependence, and harmonics.

Code	Beam	Dim.	Time	Harm.
Fast[5]	Particles	3D	Yes	No
Felex[6]	Particles	3D	Yes	No
Felos[7]	Particles	3D	Yes	Yes
Fels[8]	Particles	3D	No	No
Fred3D[9]	Particles	3D	No	No
FS1T[10]	Collective	1D	Yes	No
Genesis 1.3[11]	Particles	3D	Yes	No
Ginger[12]	Particles	2D	Yes	No
Medusa[13]	Particles	3D	No	Yes
Nutmeg[14]	Particles	2D	No	Yes
Perseo[15]	Particles	1D	Yes	Yes
Prometeo[16]	Particles	1D	No	Yes
Ron[17]	Collective	3D	Yes	No
Sarah[18]	Collective	1D	Yes	No
TDA3D[19]	Particle	3D	No	Yes

Table 1 lists the features of several Free-Electron Laser codes. A beam description by collective variables allows a faster calculation time but the validity of the output is limited to the start-up and linear regime of the FEL. Similar, a SASE FEL process can only be simulated when the codes covers time-dependent variation of the electron beam and radiation field.

In the following sections we describe the core algorithm of a FEL code and the additional problems of time-dependent simulation. With the ongoing effort to better predict the FEL output the simulations has been extended to cover the entire process from the generation of the electron bunch to the delivery of the FEL radiation to the experimental station, where the FEL process is only a part of the start-end simulation [22]. The last section covers this

final topic.

CORE ALGORITHM

With a few exceptions, the fundamental assumption of all Free-Electron Laser simulation codes is that the interaction between the electrons and the radiation field is negligible over one undulator period. A significant effect has to be accumulated over many periods, restricting the interaction to a narrow frequency bandwidth around the resonant wavelength of the Free-Electron Laser. The electron motion is averaged over one undulator period, eliminating the requirement to resolve each period with multiple integration steps. In fact, the integration step size can be chosen to be a fraction of the gain length [23] of the Free-Electron Laser. This is beneficial for short wavelength FELs, where the number of undulator periods is large in comparison to a long wavelength FEL, but the number of gain lengths and, thus, the number of integration steps remains the same.

The natural selection of a narrow bandwidth due to the resonance approximation, allows to expand the radiation field around the dominant oscillation $\exp[ik(z-ct)]$, where k is the wave number of the resonance wavelength. The change in the field amplitude A is small compared to this oscillation and the field equation is simplified by the paraxial approximation to

$$\left[\vec{\nabla}^2 - 2ik\left(\frac{\partial}{c\partial t} + \frac{\partial}{\partial z}\right)\right] A = -\frac{e^2\mu_0}{m} f_c a_u \left\langle \frac{e^{-i\theta}}{\gamma} \right\rangle \quad , \tag{1}$$

where f_c is the coupling coefficient between the electron beam and the radiation field, a_u is the undulator parameter, γ is the electron energy and $\theta = (k + k_u)z - ct$ is the ponderomotive phase of the electron with k_u as the undulator wavenumber and μ_0 as the magnetic permeability.

Because the continuous amplitude A cannot be described numerically in full detail, the field is either represented by a finite set of grid points or a set of orthonormal functions. The first approach is the most common and the field equation is solved by standard Finite-Difference methods [24].

For SASE FELs, which starts from the spontaneous radiation at the beginning of the undulator, the source term in the right hand side of Eq. 1 has strong fluctuations in the transverse direction before the process of transverse coherence smooth out the transverse bunching profile. In this initial stage many higher modes couple with the beam with almost equal strength. Thus, the growth rate in the calculated power depends strongly on the number of available modes or grid points. This artifact arises from the fact that the integration step size and the grid size determines the frequency interval and solid angle in which the spontaneous radiation is emitted [25]. In the limit of infinitely small step sizes and grid spacing the full power of the spontaneous radiation would be included by the simulations. For X-ray FELs, the initial power level of the higher modes can mask the exponential growth of the spontaneous radiation emitted in the coherent solid angle of the FEL radiation. Fig. 1 shows the evolution of the radiation power in the near field for the 3D code Genesis 1.3 and the 2D code Ginger. The difference in the power level of these codes is apparent. The number of modes is about a factor of 200 higher in Genesis 1.3 than in Ginger. The amount of total power for the 3D case is in good agreement with the theory ([25]).

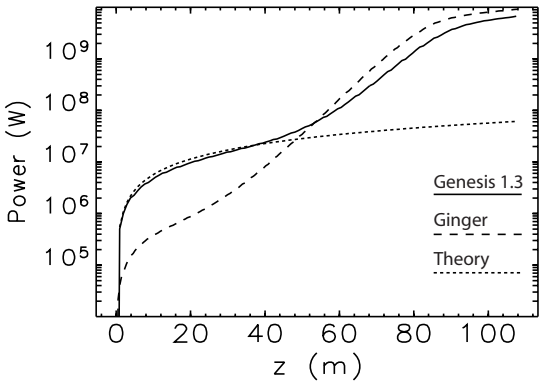

Figure 1: Radiation power in near field zone for the 3D code Genesis 1.3, the 2D code Ginger and the theoretically resolved power, using the grid dimension and integration step size as in the Genesis 1.3 run.

The integration of the equations of motion for the macro particles, resembling the phase space distribution of the electron beam, typically uses a simple and stable solver such as 4th order Runge-Kutta or Predictor-Corrector methods [26]. External effects such as wake fields [27] or the energy loss due to the emission of the spontaneous radiation [28] are applied by pre-calculated values or analytical formulae. A self-consistent description would render the calculation speed of the highly specialized case of the Free-Electron Laser interaction intractable.

For SASE simulations the codes must supply the correct statistics in the current fluctuation of the electron bunch. Averaging over many shots, the phase of the bunching factor $b =< \exp[i\theta] >$ should be a uniform distribution, while the absolute square follows a negative exponential distribution, with a mean value of the inverse of the number electrons [29]. The number of macro particles is typically much smaller than the number of electrons to be modelled. Pure random phases of the macro particles would yield too strong of fluctuation in the current and, thus, too high emission levels of the spontaneous radiation.

To avoid the noise statistics problem the loading of the phase space distribution is split into three steps. The first step fills all dimensions except for the ponderomotive phase, which is equivalent to the longitudinal position. Typically a quiet start method [30] is applied, based on the generalize bit-reverse technique of the Halton sequence [31].

In the second step the longitudinal phase is added, either by an equidistant distribution, a random number generator or a Halton sequence, but it fills only one out of n_b bins in the ponderomotive phase between 0 and 2π. Then

the entire 6D distribution is copied into the remaining bins. Each macro particle and its $n_b - 1$ mirror particles form a beamlet. The bunching factor of each beamlet is ensured to be zero due to the mirror procedure. The choice of n_b also determines the validity of the higher harmonics in the bunching factor. The calculated value is physically meaningful only for harmonics n_h up to $n_h < (n_b - 1)/2$ [33]. Therefore the minimal requirement is four bins if only the fundamental radiation ($n_h = 1$) is considered in the simulation.

The last step models the fluctuations in the particle positions. The Penman algorithm [32] adds a random offset from a uniform distribution to each macro particle. The width of the uniform distribution depends on the number of electrons to be simulated. A further improvement is the method of complex harmonic phasors [33], which also reproduces the correct statistic for the higher harmonics in the bunching factor.

Fig. 2 shows the basic flow diagram for the majority of FEL codes. Steady-state codes have the grey parts omitted.

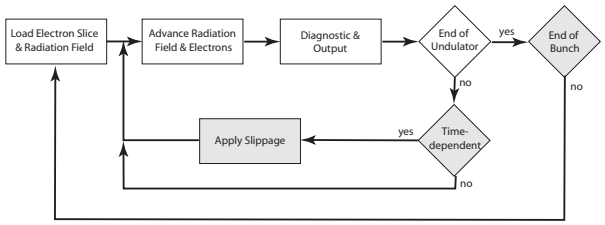

Figure 2: Algorithm for FEL simulations. Additions for time-dependent simulations are marked with grey boxes.

TIME-DEPENDENT SIMULATION

A computationally efficient method is the steady-state simulation, where any longitudinal variation in the electron beam parameter of radiation field is excluded. However, the efficiency comes at a price: less physics is included. The simulation covers only a single slice with a thickness of one radiation wavelength. The effect of slippage is not sufficiently covered because the periodic boundary condition in the longitudinal direction feeds the forward propagating radiation field back into the same slice.

Any simulation of longitudinal variation in the electron beam, including the initial fluctuation of the electron positions for the SASE operation of an FEL, require incorporating slippage effects in the simulation. For this purpose the electron bunch and the radiation field are sampled with multiple slices of constant spacing. A fully consistent description would keep all slices in the memory at once. Because each slice has about 10000 macro particles and the total number of slices can easily exceed 100000 for short wavelength FELs, the high memory demands could only be fulfilled by a massive parallel computer architecture.

The memory problem is solved by assuming a "quasi"-periodic situation of the radiation field and electron beam. The simulation is split into steady-state simulation over a short subsection of the undulator and advancing the radiation field to the next electron slice. For a giving spacing Δt the length of the steady-state integration is $\Delta z = (\lambda_u/\lambda)c\Delta t$. Because the information is propagated only in the forward direction, the simulation can start with the first electron slice at the tail of the electron bunch. After each integration length Δz the radiation field is temporary stored in memory or on the hard disk. After the slice is fully propagated through the undulator, the next electron slice is loaded and seeded with the radiation field in memory. The radiation field is again stored for the next slice after the integration distance Δz. Using this method the number of slices do not impose a limit on the memory. The maximum required information is the sampled radiation field with a spacing of Δt over the full slippage length of the FEL.

This sequential integration along the electron bunch from the tail to the head introduces several restrictions for the validity of the simulation:

First a strong impact of steady-state integrations has to be avoided by a frequent advance of the radiation field. Typically the occurring spikes in the radiation profile have to be resolved with enough slices, which is equivalent to the statement that Δz has to be much smaller than the FEL gain length or that the sampling of the radiation field can resolve the entire FEL bandwidth in the frequency domain.

Second, the seeding for the first slice is unknown if only a subsection of the electron bunch is simulated. This results in invalid field values over the first slippage length. Therefore the total time window – the product of the number of slices and the spacing Δt – must be larger than the slippage length.

Third, the gain is reduced if the mean energy of the electron slice deviates from the resonant energy of the central wavelength, as it is the case of an electron beam with an energy chirp [34]. The problem is solved by a smaller spacing of the slices, which is equivalent to a larger frequency bandwidth of the FEL simulation.

START-END SIMULATION

The initial conditions of the electron beam or radiation beam are often more complicated than are described by a few parameters such as mean and rms values of the 6D phase space distribution. In addition, X-ray Free-Electron Lasers have co-operation lengths [35] shorter than the bunch length. Different parts of the bunch amplify the radiation independently. Projected quantities such as the emittance of energy spread loose the merit of describing the beam. Instead sliced values are of relevance with a slice thickness given by the co-operation length. Fig. 3 shows the input phase space distribution for the LCLS X-ray FEL and the output radiation profile of the FEL from a start-end simulation. The shape of the distribution denies a parameterization of the beam profile with mean energy and energy spread values, because the FEL performance depends critically on the explicit shape of the distribution in energy.

To predict the performance of a Free-Electron Laser requires an effort to model the entire FEL process, starting from the electron bunch creation to the experimental station for the laser light. Because the entire process cannot be simulated by a single code, a chain of specialized codes are used. The interface between the codes is the exchange of entire particle or field distributions, or if the distribution is simple enough, a list of mean and rms values of the distribution.

The following is a list of the major components of the start-end simulation chain and the emphasize of the physical/numerical problems, addressed by the codes. The codes, listed here, have been used in context of modelling existing and future Free-Electron Lasers.

In the rf photo electron gun the electrons experience a strong acceleration from being at rest to a highly relativistic motion. The space charge forces of the generated electron beam determines the slice emittances. Point-point calculation scales with the square of the macro particle numbers, which imposes a limit for the acceptable number of particles. RF gun codes execute faster when the space charge field is evaluated on a grid. The grid filters out high frequency components, which would otherwise yield a stringent restriction on the integration step size. The particles are tracked to an energy, where the space charge field has a negligible impact. Codes, already successfully used in start-end simulations, are PARMELA [36] and ASTRA [37].

The propagation of the beam through the linac uses standard tracking methods such as matrix multiplication, including higher order effects. The support of wakefields are essential for a complete simulation of the beam transport. The overall execution time is fast compared to other codes in the start-end simulation, but due to the large set of input parameters such as field strength of each magnet or the phase and amplitude of each rf cavity, the optimization process is rather complex. Due to its scripting capability, ELEGANT [38] is useful tool for this task.

Although ELEGANT has an analytical model of the coherent synchrotron radiation [39] in a bend, the process of bunch compression in a magnetic chicane can be calculated in more detail with the specialized code Trafic4 [40]; the price is an execution time comparable to time-dependent FEL simulations.

Time-dependent simulations have been described in the previous chapter. For a complete picture of the beam dynamics within the undulator, the following processes should be included in the simulations: undulator wakefields, energy loss by the emission of spontaneous radiation, the increase of the energy spread due to the quantum fluctuation [41] in the emission of spontaneous radiation. The codes FAST, GINGER and GENESIS 1.3 are capable of modeling the above and are used in a start-end simulation.

The incorporation of the propagation of the FEL radiation through the beam line optics is currently under development [42]. Various programs exist, which can advance a single amplitude/phase front of the output radiation. However the output of time-dependent FEL codes is a lattice of these wavefronts, creating a 3D grid of the radiation field. Optical elements such as gratings or monochromators would require the Fourier transformation, the calculation of the Green's function for the optical element and then the inverse Fourier transformation to get back the field information in time domain. While the time-dependent FEL simulations sequentially calculate the radiation field without having the entire field in memory, it is essential for the Fourier transformations. To limit the memory demand a filter function might be necessary to reduce the amount of information in the field.

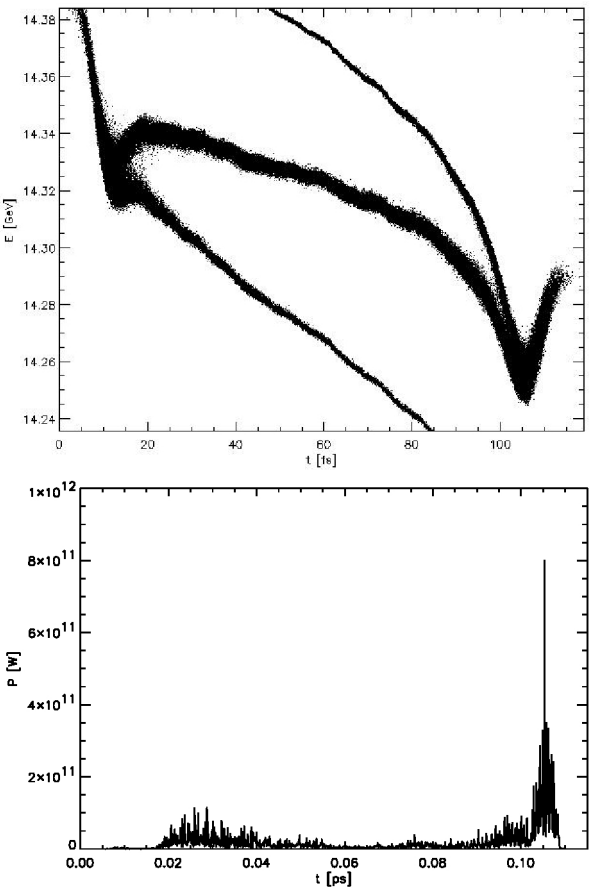

Figure 3: Initial phase space distribution at the entrance of the LCLS undulator (top graph) and radiation profile at the exit of the FEL (bottom graph), based on a start-end simulation for the LCLS X-ray FEL.

CONCLUSION

Numerical tools are invaluable for the modeling of high-gain Free-Electron Lasers, because they extend the capability to model realistic cases with many input parameters. The algorithm deviates from standard PIC codes due to the extreme scale of the FEL process. While the undulator

length is up to 100 m long, the field and electron distribution has to be resolved on a sub-Ångstrom level.

Various FEL codes exist, following similar approachs to model the FEL interaction. With the ongoing growth in computational speed and memory, the codes have become capable of handling more complex cases with a finer detail of description and more macro particles and grid points.

Besides the continuous improvement in the algorithm of the FEL codes, the interface with other accelerator/non-FEL codes has been improved. This allows to simulate the entire process, starting from the rf gun to experimental station, using the FEL light. However, these start-end simulations are complex and require an experienced user for each code in the simulation chain.

REFERENCES

[1] A.M. Kondradenko and E.L. Saldin, Part. Accel. **10** (1980) 207; R. Bonifacio, C. Pellegrini, and L.M. Narducci, Opt. Comm. **50** (1984) 373

[2] *Linac Coherent Light Source (LCLS)*, SLAC-R-521, UC-414 (1998) and *TESLA - Technical Design Report*, DESY 2001-011, ECFA 2001-209, TESLA Report 2001-23, TESLA-FEL 2001-05, Deutsches Elektronen Synchrotron, Hamburg, Germany (2001)

[3] L.-H. Yu *et al.*, Phys. Rev. Lett. **64** (1990) 3011

[4] e.g. R.L. Elias *et al.*, Phys. Rev. Lett. **36** (1976) 717; M. Hogan *al.*, Phys. Rev. Lett. **81** (1998) 4867; V. Ayvazyan *et al.*, Phys. Ref. Lett. **88** (2002) 104802

[5] E.L. Saldin, E.A. Schneidmiller, M.V. Yurkov, Nucl. Inst. & Meth. **A429** (1999) 233

[6] B.D. McVey, Nucl. Inst. & Meth. **A250** (1986) 449

[7] Private Communication with Z. Weng, Y. Shi

[8] D. Nölle, DELTA Int. Rep. 91-13, Dortmund, Germany, 1991

[9] E.T. Scharlemann, J. Appl. Phys. **58(6)** (1985) 2154

[10] Private Communication with E.L. Saldin, E.A. Schneidmiller, M.V. Yurkov

[11] S. Reiche, Nucl. Inst. & Meth. **A429** (1999) 243

[12] W.M. Fawley, *An Informal Manual for GINGER and its Post-processor XPLOTGIN*, LBID-2141, CBP Tech Note-104, UC-414, 1995

[13] H.P. Freund, T.M. Antonsen, Jr., *Principles of Free-electron Lasers*, 2nd Edition. Chapman & Hall, London, 1986, Phys. Rev. **E 52** (1995) 5401

[14] E.T. Scharlemann and W.M. Fawley, **SPIE 1045** (1989) 18

[15] L. Gianessi, Proc. of the 27th Advanced ICFA Beam Dynamics Workshop, Cagliari, Sardinia, Italy (2002)

[16] G. Dattoli, M. Galli, and P.L. Ottaviani, ENEA Internal Report No. RT/INN/93/09

[17] R.J. Dejus, O. Shevchenko, N. Vinokurov, Nucl. Inst. & Meth. **A429** (1999) 225

[18] Private Communication with P. Pierini

[19] T.M. Tran,J.S. Wurtel, Computer Physics Communicationd **54** (1989) 263

[20] C. Pellegrini *et al*, Nucl. Inst. & Meth. **A475** (2001) 328

[21] B.M. Kincaid, J. Opt. Soc. Am. **B2** (1985) 1294

[22] M. Borland *et al*, Nucl. Inst. & Meth. **A483** (2003) 268

[23] E.L. saldin, E.A. Schneidmiller, and M..V. yurkov, *the Physics of Free Electron Lasers* (Springer - Berlin - 2000)

[24] W.F. Ames, *Numerical Methods for Partial Differential Equations* (Academic Press - New York - 1969)

[25] Z. Huang, Proc. of the 24th Free-Electron Laser Conference, Argonne, USA, 2002

[26] W.H. Press *et al.*, *Numerical Recipes* (Cambridge University Press - Cambridge - 1986)

[27] S. Reiche and H. Schlarb, Nucl. Inst. & Meth. **A445** (2000) 155

[28] J.D. Jackson, *Classical Electrodynamics* (John Wiley and SOns - New York - 1975)

[29] J. Goodman, *Statistical Optics* (John Wiley and Sons - New York - 1985)

[30] T.M. Tran and J.S. Wurtele, Comp. Phys. Comm. **54** (1989) 263

[31] J.H. Halton, Numerische Mathematik **2** (1960) 84

[32] C. Penman and B.W.J. McNeil, Opt. Comm. **80** (1992) 82

[33] W.M. Fawley, Phys. Rev. STAB **5** (2002) 070701

[34] W.M. Fawley, Proc. of the 24th Free-Electron Laser Conference, Argonne, USA, 2002

[35] R. Bonifacio *et al.*, Phys. Rev. Lett. **73** (1994) 70

[36] J. Billen, PARMELA, Los Alamos National Laboratory report LA-UR-96-1835, 1996

[37] K. Flöttmann, Astra User Manual, *http://www.desy.de/ mpyflo/*

[38] M. Borland, Argonne National Laboratory Report LS-287, 2000

[39] Y.S. Derbenev, J. Rossbach, E.L. Saldin and V.D. Shiltsev, TESLA-FEL 95-05, Deutsches Elektronen Synchrotron, Hamburg, Germany

[40] A. Kabel, M. Dohlus and T. Limberg, Nucl. Inst. & Meth. **A445** (2000) 338

[41] E.L. Saldin *et al*, Nucl. Inst. & Meth. **A381** (1996) 545

[42] Private Communication with R. Bionta